Kinetochore localisation and phosphorylation of the mitotic checkpoint components Bub1 and BubR1 are differentially regulated by spindle events in human cells

Stephen S. Taylor, Deema Hussein, Yunmei Wang[1], Sarah Elderkin* and Christopher J. Morrow

School of Biological Sciences, University of Manchester, 2.205 Stopford Building, Oxford Road, Manchester M13 9PT, UK
[1]Department of Biological Chemistry and Molecular Pharmacology, Harvard Medical School, 240 Longwood Avenue, Boston MA 02115, USA
*Present address: Department of Biology, Imperial College of Science Technology and Medicine, London SW7 2AZ, UK
Author for correspondence: stephen.taylor@man.ac.uk

Accepted 6 September 2001
Journal of Cell Science 114, 4385-4395 (2001) © The Company of Biologists Ltd

SUMMARY

***BUB1* is a budding yeast gene required to ensure that progression through mitosis is coupled to correct spindle assembly. Two related human protein kinases, Bub1 and BubR1, both localise to kinetochores during mitosis, suggesting that they play a role in delaying anaphase until all chromosomes achieve correct, bipolar attachment to the spindle. However, how the activities of Bub1 and BubR1 are regulated by spindle events and how their activities regulate downstream cell cycle events is not known.**

To investigate how spindle events regulate Bub1 and BubR1, we characterised their relative localisations during mitosis in the presence and absence of microtubule toxins. In prometaphase cells, both kinases colocalise to the same domain of the kinetochore. However, whereas the localisation of BubR1 at sister kinetochores is symmetrical, localisation of Bub1 is often asymmetrical. This asymmetry is dependent on microtubule attachment, and the kinetochore exhibiting weaker Bub1 staining is typically closer to the nearest spindle pole. In addition, a 30 minute nocodazole treatment dramatically increases the amount of Bub1 localising to kinetochores but has little effect on BubR1. Furthermore, Bub1 levels increase at metaphase kinetochores following loss of tension caused by taxol treatment. Thus, these observations suggest that Bub1 localisation is sensitive to changes in both tension and microtubule attachment.

Consistent with this, we also show that Bub1 is rapidly phosphorylated following brief treatments with nocodazole or taxol. In contrast, BubR1 is phosphorylated in the absence of microtubule toxins, and spindle damage has little additional effect. Although these observations indicate that Bub1 and BubR1 respond differently to spindle dynamics, they are part of a common complex during mitosis. We suggest therefore that Bub1 and BubR1 may integrate different 'spindle assembly signals' into a single signal which can then be interpreted by downstream cell cycle regulators.

Key words: Mitosis, Spindle checkpoint, Bub1

INTRODUCTION

Before cell division, the replicated genome is segregated such that the two daughter cells receive all the genetic information required for further growth and development. The fate of the daughters is dependent on the accuracy of this process as chromosome mis-segregation alters gene dosage and can therefore result in cell death, the evolution of cancer cells and diseases such as Down's syndrome (Nicklas, 1997). To maintain accuracy and thus ensure that both daughters receive one copy of each chromosome, eukaryotes have evolved a surveillance mechanism that coordinates spindle assembly with the initiation of anaphase (Amon, 1999).

How anaphase is initiated is now well understood, at least in budding yeast (Nasmyth, 1999). Following chromosome alignment, the Cdc20 protein is activated, resulting in the activation of an E3 ubiquitin ligase, the anaphase promoting complex/cyclosome (APC/C). An APC/C substrate, Pds1/Cut2 securin, is subsequently ubiqutinated then degraded by the 26S proteosome, resulting in activation of the Esp1/Cut1 seperase, which in turn cleaves the Scc1 cohesin. Sister chromatid cohesion is abolished and anaphase initiates. Although this model describes how anaphase starts, our understanding of the mechanisms that inhibit anaphase before chromosome alignment remains far from complete.

It has been suspected for many years that kinetochores play a key role in regulating anaphase onset (Zirkle, 1970). More recently, an analysis of mitotic PtK_1 cells showed that a single mono-oriented chromosome can delay anaphase for hours (Rieder et al., 1994). However, when the unattached kinetochore on the last mono-oriented chromosome was selectively destroyed by laser ablation, anaphase initiated with normal kinetics (Rieder et al., 1995). Thus, unattached kinetochores appear to generate signals that inhibit the machinery required for dissolving sister chromatid cohesion. Whether attachment of kinetochores to microtubules

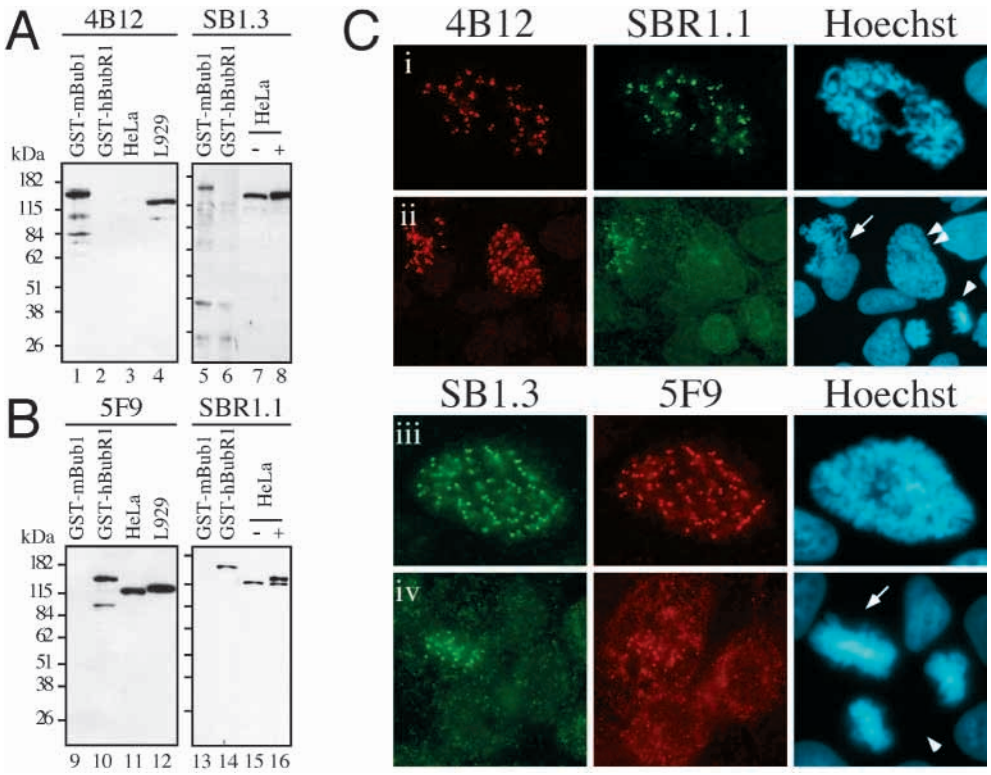

Fig. 1. Characterisation of antibodies against Bub1 and BubR1. (A and B) Protein extracts from BHK cells ectopically expressing either GST-mBub1 (lanes 1, 5, 9 and 13) or GST-BubR1 (lanes 2, 6, 10 and 14), TA-HeLa cells (lanes 3, 7, 8, 11, 15 and 16) and mouse L929 cells (lane 4 and 12) analysed by western blotting with (A) the anti-Bub1 antibodies 4B12 (mouse monoclonal) and SB1.3 (sheep polyclonal) and (B) the anti-BubR1 antibodies 5F9 (mouse monoclonal) and SBR1.1 (sheep polyclonal). Where indicated, HeLa cells were either asynchronous (–) or treated with 0.2 μg/ml nocodazole for 16 hours (+). (C) Immunofluorescence images of DLD-1 cells stained with monoclonal (red) and polyclonal (green) antibodies against Bub1 (left column) and BubR1 (middle column). The cells were also stained with Hoechst to identify the chromosomes (blue, right column). (i, iii) Late prophase cells showing colocalisation of Bub1 and BubR1 at kinetochores. (ii, iv) Fields showing multiple mitotic cells. Note that in anaphase cells (arrowheads), Bub1 and BubR1 are virtually undetectable at kinetochores yet at prometaphase (ii) and metaphase (iv) cells (arrows) kinetochore-associated Bub1 and BubR1 is clearly detectable. Note also that in early prophase (double arrowhead) Bub1 localises to kinetochores before BubR1.

downregulates the anaphase inhibiting signal in all cell types remains to be seen. Micromanipulation of chromosomes in mantid spermatocytes suggests that it is the application of tension across kinetochores which signals the 'all clear' for anaphase (Li and Nicklas, 1995).

In budding yeast, inhibition of premature anaphase is dependent on the spindle checkpoint components Bub1, Bub3, Mad1, Mad2 and Mad3 (Hoyt et al., 1991; Li and Murray, 1991). Significantly, prior to chromosome alignment, it is now clear that Mad2 binds and inhibits Cdc20 (Fang et al., 1998; Hwang et al., 1998; Kim et al., 1998), explaining how an active spindle checkpoint pathway inhibits anaphase. However, although it is known that the yeast spindle checkpoint components form a variety of complexes with each other (Brady and Hardwick, 2000; Hardwick et al., 2000), it is still not known how spindle events regulate the activities of these molecules.

In higher eukaryotes, Bub1, Bub3, Mad 1, Mad2 and a Bub1/Mad3-related protein called BubR1 localise to kinetochores during mitosis, consistent with the notion that they monitor the attachment of kinetochores to the spindle (Chen et al., 1996; Li and Benezra, 1996; Taylor and McKeon, 1997; Basu et al., 1998; Chan et al., 1998; Chen et al., 1998; Jablonski et al., 1998; Taylor et al., 1998; Basu et al., 1999; Chan et al., 1999; Sharp-Baker and Chen, 2001). Interestingly, Bub1 and BubR1 are protein kinases, and in budding yeast Bub1 kinase activity is required for checkpoint function (Roberts et al., 1994). Evidence that kinetochore phosphorylation plays a role in regulating anaphase comes from the observation that unattached kinetochores are recognised by the phospho-specific antibody 3F3/2 (Gorbsky and Ricketts, 1993). In contrast, attached kinetochores are not recognised by this antibody. Injection of 3F3/2 into mitotic cells delays anaphase, suggesting that kinetochore dephosphorylation is required for checkpoint inactivation (Campbell and Gorbsky, 1995). Significantly, when tension was artificially applied to kinetochores in grasshopper spermatocytes, it reduced 3F3/2 phosphorylation (Nicklas et al., 1995). In addition, loss of tension across kinetochores following taxol treatment of PtK1 cells resulted in kinetochore re-phosphorylation (Waters et al., 1998), suggesting that tension may also play a role in mammalian somatic cells. Thus, although kinetochore phosphorylation appears to be sensitive to changes in tension, how tension and/or microtubule attachment regulate the activities of the Bub and Mad proteins is still unknown (Shah and Cleveland, 2000).

It is now known that changes in microtubule attachment and tension can effect the localisation of spindle checkpoint proteins to kinetochores. Specifically, Mad2 is lost from PtK_1 kinetochores as they accumulate microtubules, and it re-binds previously attached kinetochores upon nocodazole-induced microtubule depolymerisation (Waters et al., 1998). Mad2 does not re-bind, however, when tension is lost owing to taxol treatment. In contrast, when HeLa cells were treated with low levels of vinblastine, thus reducing tension but not severing kinetochore microtubule interactions, Bub1 and BubR1 re-accumulated at kinetochores (Skoufias et al., 2001).

Further insight into how the activity of BubR1 might be

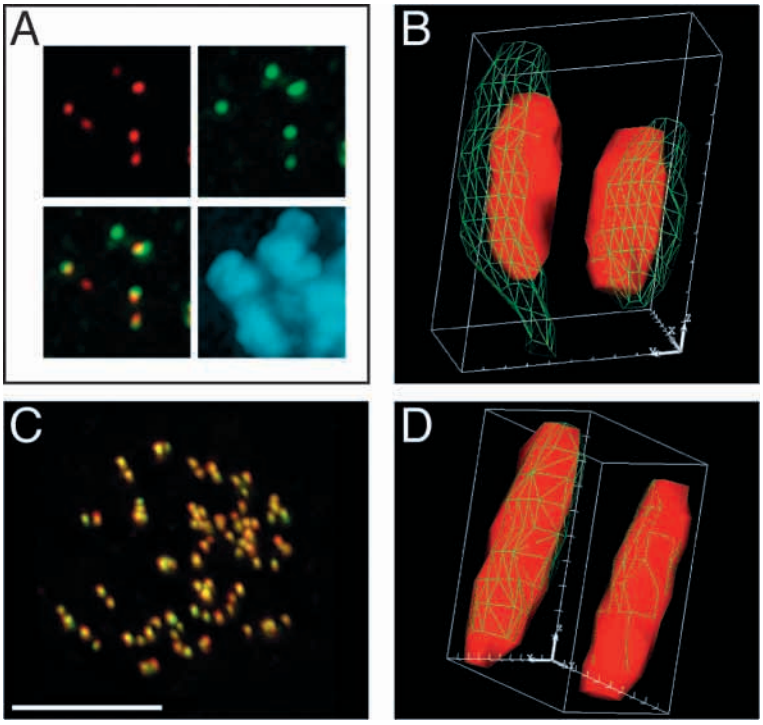

Fig. 2. Bub1 and BubR1 localise to the same domain within the kinetochore. (A) Projection of a deconvoluted image stack showing DLD-1 prometaphase kinetochore pairs stained with 4B12 (anti-Bub1, red) and RCE1 (anti-Cenp-E, green), showing that localisation of Cenp-E extends distally beyond Bub1. (B) 3D model showing that Cenp-E also extends beyond Bub1 in the z axis. (C) Projection of a deconvolved image stack showing a nocodazole-treated DLD-1 cell stained with 4B12 (anti-Bub1, red) and SBR1.1 (anti-BubR1, green). Because Bub1 and BubR1 colocalise perfectly the kinetochores appear orange in this merged image. Scale bar represents 5 μm. (D) 3D model of one of the kinetochores from (C) showing perfect overlap of Bub1 and BubR1.

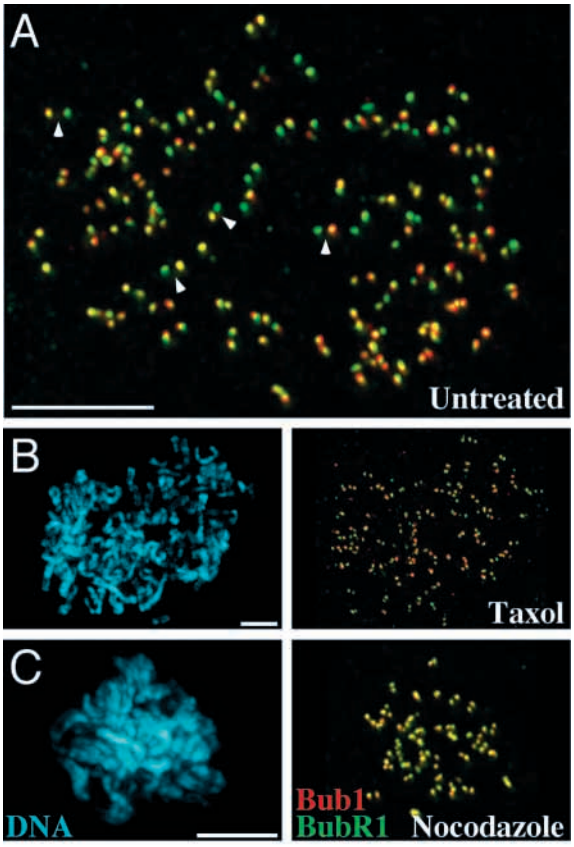

Fig. 3. Sister kinetochores exhibit asymmetric Bub1/BubR1 staining. Projections of deconvoluted image stacks showing DLD-1 cells stained with 4B12 (anti-Bub1, red), SBR1.1 (anti-BubR1, green) and Hoechst (blue). Scale bars represent 5μm. (A) Merged red/green image of an untreated cell showing that one kinetochore within a pair often appears green while the other appears orange/yellow, indicative of asymmetric Bub1/BubR1 staining. The arrowheads identify four clear examples. (B) A taxol-treated cell, showing splayed-out chromosomes due to microtubule stabilisation, also exhibits asymmetric Bub1/BubR1 staining. (C) A nocodazole-treated cell, showing collapsed chromosomes owing to microtubule depolymerisation, exhibits reduced Bub1/BubR1 asymmetry: most of the kinetochores appear orange/yellow.

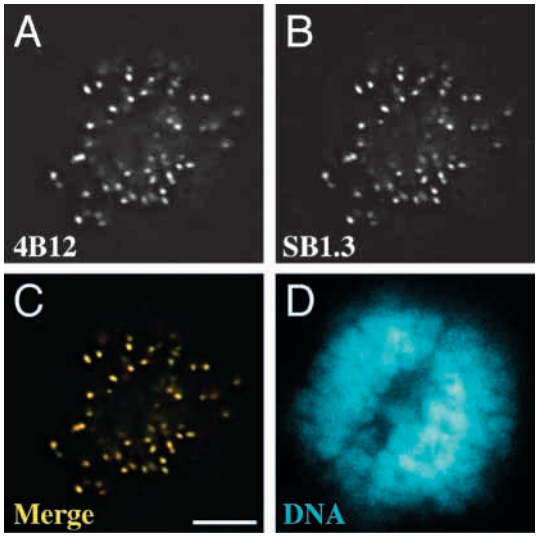

Fig. 4. Monoclonal and polyclonal anti-Bub1 antibodies give identical patterns. A deconvolved image of a prometaphase DLD-1 cell stained with (A) 4B12 and (B) SB1.3 anti-Bub1 antibodies. (C) shows a red/green merged image and (D) shows the Hoechst-stained chromosomes. The scale bar represents 5 μm. Both 4B12 and SB1.3 give identical patterns.

coupled with spindle events comes from the observation that BubR1 interacts with the kinesin-related protein Cenp-E (Chan et al., 1998). Significantly, disruption of Cenp-E function delays anaphase onset (Chan et al., 1999; Yao et al., 2000). Furthermore, inhibition of BubR1 function in Cenp-E-defective cells abrogates this mitotic block (Chan et al., 1999). Although these observations suggest that Cenp-E is required for checkpoint inactivation, it has also been demonstrated that Cenp-E is required for chromosome congression (Schaar et al., 1997; Wood et al., 1997). Thus, it is possible that disruption of Cenp-E interferes with kinetochore-microtubule interactions, activating the checkpoint and inducing mitotic arrest.

Although significant progress has been made in identifying the molecules required to prevent premature anaphase, many

unanswered questions remain. In particular, why do mammals express two Bub1-related protein kinases? Do these two kinases respond to different spindle events? Do they relay different signals to downstream cell cycle effectors? To begin to address these issues, we have carried out a comparative analysis of Bub1 and BubR1 in human cells. We show that Bub1 and BubR1 behave differently, both in terms of their localisation patterns and their biochemical behaviour during mitosis. Although these observations suggest that Bub1 and BubR1 monitor different spindle events, we also find that they are part of a common complex in checkpoint-activated cells, raising the possibility that Bub1 and BubR1 integrate different signals into a single signal that is then relayed to the downstream cell cycle machinery.

MATERIALS AND METHODS

Cell culture and drug treatment

TA-HeLa, L929 cells and NOS myeloma cells were used, as described in (Taylor and McKeon, 1997). Human DLD-1 cells and BHK cells were obtained from the ATCC. All lines were cultured in a humidified incubator at 37°C plus 5% CO_2 in Dulbecco's modified Eagle's media (DMEM) supplemented with 10% fetal calf serum, 100 U/ml penicillin, 100 μg/ml streptomycin and 2 mM glutamine. For monoclonal antibody production, fusions were plated in DMEM with 20% serum (Sigma CPSR-3), 5% NCTC, 1% non-essential amino acids, 2 mM glutamine, 100 U/ml penicillin, 100 μg/ml streptomycin and 1 x HAT. All tissue culture reagents were from GIBCO BRL unless stated otherwise. Nocodazole (Sigma, 5 mg/ml in DMSO) and taxol (Sigma, 10 mM in DMSO) were freshly diluted in media and used at final concentrations of 0.2 μg/ml and 10 μM respectively. To completely depolymerise microtubules, cells were incubated with nocodazole on ice for 30 minutes then returned to 37°C for a further 30 minutes in the presence of nocodazole. To synchronise TA-HeLa cells in early S phase, a standard double thymidine block-and-release protocol was used (Taylor and McKeon, 1997).

Generation of antibodies

cDNA fragments encoding portions of human Bub1 (amino acids 336-489) and BubR1 (amino acids 2-422 and 2-211) (Taylor et al., 1998) were amplified using Pfu polymerase (Stratagene) then cloned into pGEX-4T-3 (Pharmacia) as BamHI/NotI restriction fragments. GST fusion proteins were expressed in BL21 *Escherichia coli* cells by induction with 1 mM IPTG at 37ºC then purified using glutathione Sepharose beads (Pharmacia) according to the manufacturers instructions. The anti-BubR1 monoclonal antibody, 5F9, was generated following procedures described previously (Taylor and McKeon, 1997). Briefly, mice were immunised with GST-BubR1(2-422). Spleenocytes from mice with positive immune responses were isolated, fused with myeloma cells and the resulting hybridomas screened by ELISA for reactivity against recombinant BubR1(2-422). One positive hybridoma, 5F9, was expanded, the tissue culture supernatant harvested and used for all subsequent experiments. The anti-Bub1 and anti-BubR1 sheep polyclonal antibodies, SB1.3 and SBR1.1, respectively, were generated by immunisation of sheep (Scotland Diagnostics Ltd) with GST-Bub1 (336-489) and GST-BubR1(2-211), respectively, followed by affinity purification using standard procedures. Briefly, GST-fusion proteins were covalently coupled to Sepharose beads (Pharmacia) then incubated with crude serum and washed. Bound antibodies were eluted with 0.2M glycine at pH 2.8. Eluted antibodies were neutralised and diluted to 1 mg/ml in PBS (140 mM NaCl, 2.7 mM KCl, 10 mM Na_2HPO_4, 1.8 mM KH_2PO_4, pH 7.4). Anti-GST antibodies were then removed by incubating with Sepharose beads coated with GST.

Immunocytochemistry and fluorescence microscopy

5 x 10^4 cells were seeded on 19mm glass coverslips, cultured for 24 to 48 hours then fixed for five minutes at room temperature in 1% formaldehyde, freshly diluted from a 40% stock in PBS. Following washes in PBS plus 0.1% Triton X-100 (PBST), the cells were blocked in PBST plus 5% non-fat dried milk for 20 minutes then incubated for 30 minutes with combinations of primary antibodies diluted in PBST as follows: 4B12 [mouse anti-Bub1, (Taylor and McKeon, 1997)] 1:10; SB1.3 (sheep anti-Bub1), 1:1000; 5F9 (mouse anti-BubR1), 1:50; SBR1.1 (sheep anti-BubR1), 1:1000; RCE.1 (rabbit anti-Cenp-E, kindly provided by Don Cleveland), 1:2000; ACA (human anti-centromere antibody) 1:2000; RAA.1 (rabbit anti-aurora a, kindly provided by Nick Keen) 1:2000. Following washes in PBST, the cells were incubated with appropriate combinations of the following secondary antibodies, all diluted 1:500 in PBST: Cy3 donkey anti-mouse, Cy3 donkey anti-sheep, Cy2 donkey anti-sheep, Cy2 donkey anti-rabbit, Cy2 donkey anti-human (all from Jackson Immunoresearch). Following washes in PBST, the cells were stained with Hoechst 33258 at 1μg/ml in PBST and mounted in 90% glycerol plus 20 mM Tris HCl pH 8.0. For standard analysis, cells were viewed on a Leica DMRXA equipped with epifluorescence using a 100× objective and images captured using a Photometrics cooled CCD camera driven by IPLab software. Deconvolution microscopy was performed using a widefield optical sectioning microscope (Deltavision; Applied Precision). For each cell, a z-series of 25 to 30 images at 0.1 μm intervals was captured then processed using constrained iterative deconvolution. Deconvolved image stacks were projected and fluorescence signal intensities quantitated using SoftWorx (Applied Precision). 3D models were generated by first employing a two-dimensional polygon building algorithm. Images were then imported into Photoshop (Adobe), pseudocoloured and printed.

Transient transfections

1.6 x 10^5 BHK cells were plated in 60-mm dishes, cultured for 24 hours, then washed three times with serum-free media. 1 μg of DNA was complexed with 16 μg of Lipofectamine (GIBCO BRL) in serum-free media at room temperature for 20 minutes and then added to the cells in a final volume of 1 ml of serum-free media for 16 hours. The cells were then fed with media plus serum, cultured for a further 24 hours then scraped in SDS sample buffer.

Affinity purification of Bub1/BubR1 complexes

Soluble protein lysates were prepared by resuspending cells in lysis buffer (100 mM NaCl, 50 mM Hepes, pH 7.4, 20 mM β-glycerophosphate, 10 mM EDTA, 10 mM EGTA, 1 mM DTT, 1 mM PMSF, 1 μg/ml antipain, 1 μg/ml aprotinin, 5 μg/ml bestatin, 5 μg/ml chymostatin, 2 μg/ml leupeptin, and 1 μg/ml pepstatin), followed by centrifugation at 14,000 ***g*** for 10 min at 4ºC. To affinity purify Bub1 and BubR1 complexes, soluble protein extracts were incubated with 4B12 or SB1.3 and 5F9 or SBR1.1, respectively, for one hour at 4ºC. Immune complexes were then isolated by incubation with protein G Sepharose beads (Pharmacia) at 4ºC for 30 minutes followed by centrifugation. After five washes in 10-fold volumes of lysis buffer, proteins were eluted off the beads by boiling in SDS sample buffer.

Phosphatase treatment

To dephosphorylate Bub1, affinity-purified complexes bound to protein G beads were washed with λ phosphatase buffer supplemented with protease inhibitors then incubated with 400U λ phosphatase (NEB) at 30°C for five minutes. To dephosphorylate BubR1, protein extracts were treated with calf intestinal phosphatase (NEB) according to the manufacturers instructions for 30 minutes at 37ºC.

Western blotting

Proteins were resolved by SDS-PAGE and electroblotted onto

Immobilon-P membranes (Millipore). Blots were blocked in TBST (50 mM Tris, pH 7.6, 150 mM NaCl, 0.1% Tween-20) plus 5% non-fat dried milk overnight at room temperature then incubated with either 4B12 (1:10); SB1.3 (1:1000); 5F9 (1:50) or SBR1.1 (1:1000) in TBST. After washing in TBST, bound primary antibodies were labeled with horseradish-peroxidase-conjugated goat anti-mouse or rabbit anti-sheep antibodies (Zymed) diluted 1:500 and 1:2000 respectively in TBST. After washing in TBST, bound secondary antibodies were detected using the SuperSignal chemiluminescence system (Pierce) and imaged on Biomax MR film (Kodak).

RESULTS

Characterisation of antibodies specific for Bub1 and BubR1

To address how spindle events regulate Bub1 and BubR1, we generated several novel antibodies against recombinant Bub1 and BubR1. The anti-Bub1 monoclonal antibody, 4B12 (Taylor and McKeon, 1997), and the affinity purified anti-Bub1 sheep polyclonal antibody, SB1.3, both detect GST-mBub1 but not GST-hBubR1 (Fig. 1A). 4B12 also detects a single band of about 119 kDa, the predicted molecular weight for murine Bub1, in a total L929 cell lysate. On longer exposures, 4B12 also detects Bub1 in total HeLa cell lysates (not shown, but see Fig. 7). SB1.3 also detects a single band of about 122 kDa, the predicted molecular weight for human Bub1, in a total HeLa cell lysate. The anti-BubR1 monoclonal antibody, 5F9, and the affinity-purified anti-BubR1 sheep polyclonal antibody, SBR1.1, both detect GST-hBubR1 but not GST-mBub1 (Fig. 1B). 5F9 and SBR1.1 also detect a single band of about 120 kDa, the predicted molecular weight of hBubR1, in HeLa cell lysates. Thus, these observations suggest that 4B12 and SB1.3 recognise Bub1 but not BubR1 and conversely, 5F9 and SBR1.1 recognise BubR1 but not Bub1.

To further characterise these antibodies, human DLD-1 cells were co-stained with 4B12 plus SBR1.1, and SB1.3 plus 5F9, then analysed by fluorescence microscopy. During prophase and prometaphase, Bub1 and BubR1 clearly colocalise to kinetochores (Fig. 1C). However, during early prophase Bub1 localises to kinetochores before BubR1 (see cell labelled with double arrowhead in Fig. 1Cii), consistent with previous observations (Jablonski et al., 1998). Using both sets of antibodies, Bub1 and BubR1 are virtually undetectable at anaphase kinetochores: in Fig. 1C part ii and iv, anaphase cells are visible with little or no kinetochore-associated Bub1 or BubR1. However, in the same fields of view, Bub1 and BubR1 are clearly present at prometaphase (Fig. 1Cii) and metaphase kinetochores (Fig. 1Ciii). Thus, consistent with our previous observations (Taylor and McKeon, 1997; Taylor et al., 1998) and those of others (Chan et al., 1998; Jablonski et al., 1998), these results show that in human cells, Bub1 and BubR1 associate with kinetochores during the early stages of mitosis, but, following chromosome alignment, the amounts detectable at kinetochores are diminished.

Bub1 and BubR1 localise to the same domain within the kinetochore

The precise localisation of BubR1 and Cenp-E within the kinetochore has been determined by immunogold labelling followed by electron microscopy. Whereas Cenp-E localises to the outer plate and the corona (Cooke et al., 1997; Yao et al., 1997), BubR1 localises to the outer and inner plates (Jablonski et al., 1998). However, the exact localisation of Bub1 has not been determined. Therefore, to address whether Bub1 localises to the same domain as BubR1 or Cenp-E, we used deconvolved image stacks to generate projections and 3D models of kinetochores stained with antibodies against Bub1 and either Cenp-E or BubR1. In projections, Cenp-E appears to extend distally beyond Bub1 (Fig. 2A). This is confirmed in the 3D model (Fig. 2B), which also shows that Cenp-E extends beyond Bub1 in the z-axis. In contrast, in both projections and 3D models, the domains to which Bub1 and BubR1 localise appear to perfectly overlap (Fig. 2C and 2D). Thus, these observations suggest that Bub1 and BubR1 localise to the same domain within the kinetochore.

Sister kinetochores often appear to be asymmetric during prometaphase

Although Bub1 and BubR1 clearly colocalise to kinetochores during prometaphase, it was striking that in merged images, one kinetochore within a pair often appeared green although the other appeared orange/yellow (Fig. 3A), suggesting that the relative intensities of Bub1 and/or BubR1 varied between sister kinetochores. This asymmetry was less marked in prophase cells (not shown) suggesting that differences in microtubule occupancy at sister kinetochores might be responsible for the asymmetry. Consistently, asymmetric staining was maintained in taxol-treated cells (Fig. 3B) but appeared less marked in nocodazole treated cells (Fig. 3C).

Further analysis shows that this difference in staining is because Bub1 often localises asymmetrically to sister kinetochores in prometaphase (see below). However, in these experiments Bub1 was detected with the 4B12 monoclonal antibody, and therefore we wanted to rule out the possibility that the asymmetry was due to masking of the epitope recognised by 4B12. Therefore, we co-stained prometaphase DLD-1 cells with monoclonal and polyclonal antibodies against Bub1. Significantly, both antibodies gave identical patterns (Fig. 4), suggesting that the asymmetry observed was not due to epitope masking.

Asymmetric Bub1 staining is microtubule dependent

By analysing kinetochores that are well resolved from their neighbours, the reason for the differential staining becomes clear. Although the BubR1 signal at sister kinetochores is roughly equivalent, the Bub1 signal is often asymmetric, giving rise to a green and yellow spots in the merged image (Fig. 5A). The relative asymmetry of Bub1 is confirmed by quantifying the signal intensities at the two sister kinetochores (Fig. 5B).

To determine whether the Bub1 asymmetry correlated with microtubule-kinetochore interactions, we quantified the Bub1 and BubR1 signals at kinetochore pairs in untreated prometaphase cells and following treatment with either taxol or nocodazole. The kinetochore with greater Bub1 signal was designated ‘K1’, the other ‘K2’ and the fluorescence ratio K1/K2 calculated (Fig. 5C). In untreated cells, the Bub1 ratio at K1 relative to K2 was calculated to be 1.75±0.09 (n=115). Taxol treatment had little effect with the ratio being 1.82±0.10 (n=47). Nocodazole treatment, however, reduced the ratio to 1.31±0.05 (n=40). In contrast, the ratio of BubR1 signal at kinetochore 1 relative to kinetochore 2 was relatively

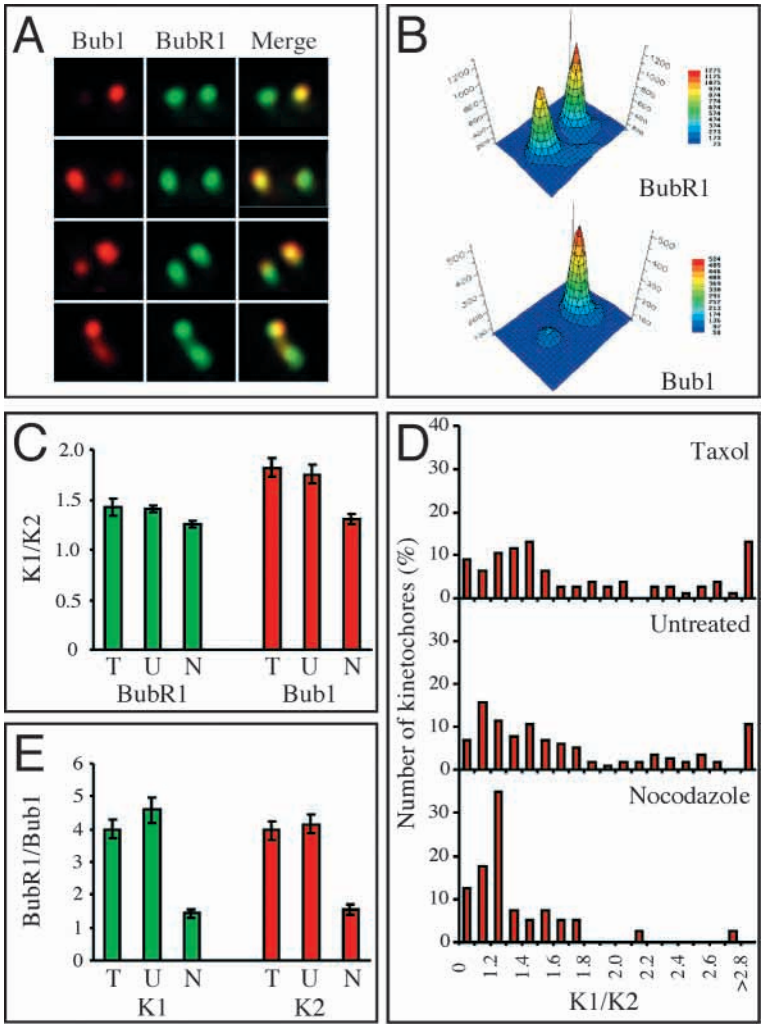

Fig. 5. Asymmetric Bub1 staining is microtubule dependent. (A) Enlarged images of kinetochore pairs taken from Fig. 3A showing Bub1 (red), BubR1 (green) and the merged image (right column). Although the BubR1 signal at sister kinetochores is roughly equivalent, the Bub1 signal is often asymmetric, giving rise to a green and yellow spots in the merged image. (B) 3D plots of a kinetochore pair confirming BubR1 symmetry and Bub1 asymmetry. (C) A bar graph plotting the fluorescence ratio (K1/K2) for Bub1 (red) and BubR1 (green) where K1 is the kinetochore within a pair exhibiting stronger Bub1 fluorescence. The cells were either untreated (U) or treated with nocodazole (N) or taxol (T) for one hour. (D) A histogram plotting the percentage of kinetochore pairs exhibiting a given K1/K2 Bub1 fluorescence ratio. (E) A bar graph plotting the average ratio of BubR1/Bub1 signal at kinetochores K1 (green) and K2 (red). Values represent the mean and the standard error of the mean (s.e.m.).

unchanged at 1.41±0.04 in untreated cells, 1.43±0.09 in taxol treated cells and 1.25±0.04 following nocodazole treatment.

Within any given cell, the extent of asymmetry varies from one kinetochore pair to another (Fig. 3A). Therefore, we also plotted histograms showing the number of kinetochores that expressed any given K1/K2 ratio (Fig. 5D). In both untreated and taxol-treated cells, the histogram peaks are low and stretch out, showing that there is a great deal of asymmetry throughout the cell. In contrast, in nocodazole-treated cells, there is a sharp peak and the tail is not as significant, showing that the asymmetry is less pronounced. Using the BubR1 data as a guide, we chose a K1/K2 ratio of less than 1.4 to signify no asymmetry and then calculated the fraction of kinetochore pairs that exhibited no Bub1 asymmetry. In untreated and taxol-treated cells, 42% and 38%, respectively, exhibited no asymmetry. In contrast, in nocodazole-treated cells, 73% of the kinetochores exhibited no asymmetry. Thus, taken together, these observations suggest that in cells where kinetochores are likely to encounter microtubules, the Bub1 staining at sister kinetochores is frequently asymmetric.

We also calculated the BubR1 to Bub1 ratio at K1 and K2 (Fig. 5E). The ratios were relatively similar in untreated (4.1±0.3 (n=115) at K2) and taxol-treated cells (4.0±0.3 (n=47) at K2). However, in nocodazole-treated cells, the ratio dropped to 1.6±0.2 (n=40) at K2, suggesting that either the BubR1 signal had reduced or the Bub1 signal had increased. Analysis of the actual fluorescence signal intensities (not shown) shows that this change in the BubR1/Bub1 ratio is due to the amount of Bub1 fluorescence increasing about three-fold while BubR1 is relatively unchanged. Thus, whereas preventing microtubule-kinetochore interactions has little effect on the amount of BubR1 at kinetochores, it dramatically increases Bub1

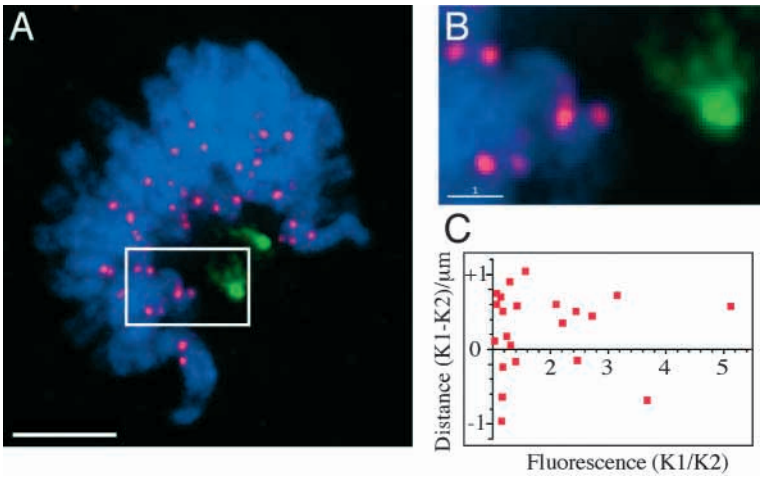

Fig. 6. Kinetochores with weaker Bub1 staining are oriented towards the spindle pole. (A) A projection of a deconvolved image stack showing a prometaphase DLD-1 cell stained with 4B12 (anti-Bub1, red), RAA.1 (anti-aurora a, green) and Hoechst (blue). (B) An enlarged image of the region boxed in (A) showing three kinetochore pairs. The two pairs that exhibit clear Bub1 asymmetry are oriented such that the weaker staining kinetochore is closer to the pole. (C) shows a dot plot of the interkinetochore distance (K1-K2) against the fluorescence ratio (K1/K2), confirming that kinetochores exhibiting weaker Bub1 staining are generally closer to the nearest spindle pole. The scale bars represent 5 μm in (A) and 1 μm in (B).

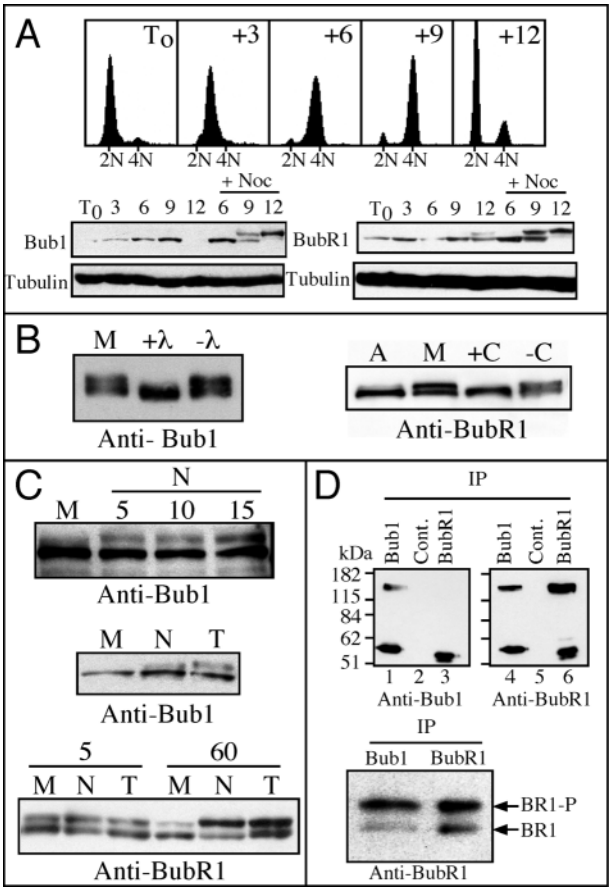

Fig. 7. Bub1 is phosphorylated in response to spindle damage. (A) HeLa cells synchronised by a double thymidine block analysed by flow cytometry (top panel) and western blotting using 4B12 (anti-Bub1, bottom left panel) and 5F9 (anti-BubR1, bottom right panel) at various times following release from G_1/S, shown in hours. The anti-tubulin antibody TAT-1 (Woods et al., 1989) was used to monitor protein loading. Between 9 and 12 hours after release, the majority of the cells had completed mitosis and returned to G_1. In the presence of nocodazole, both Bub1 and BubR1 exhibit slower migrating forms. (B) Proteins from mitotic (M) HeLa cells treated with λ phosphatase (+λ) or CIP (+C), as indicated, then blotted for Bub1 using SB1.3 or BubR1 using 5F9. Phosphatase treatment results in the disappearance of the slower migrating forms indicating that they are phosphorylated forms. (C) Mitotic L929 (M, upper panel) or mitotic HeLa cells (M, lower two panels) were treated with 0.2 μg/ml nocodazole (N) or 10 μM taxol (T) for the times indicated in minutes then blotted for Bub1 using 4B12 or BubR1 using 5F9. Phosphorylated Bub1 is only detectable in response to spindle damage but BubR1 is phosphorylated in the absence of spindle toxins. (D) Bub1 (lanes 1 and 4) and BubR1 (lanes 3 and 6) were immunoprecipitated from nocodazole-arrested TA-HeLa cells using the 4B12 and 5F9 antibodies, respectively. The immunoprecipitates were then analysed by western blotting using 4B12 (anti-Bub1, right panel) and 5F9 (anti-BubR1, left panel). The lower panel shows that when the two forms of BubR1 are well resolved, it becomes apparent that the phosphorylated form of BubR1 preferentially immunoprecipitates with Bub1.

staining. In *Xenopus* egg extracts, addition of nocodazole also increases the amount of Bub1 at kinetochores (Sharp-Baker and Chen, 2001).

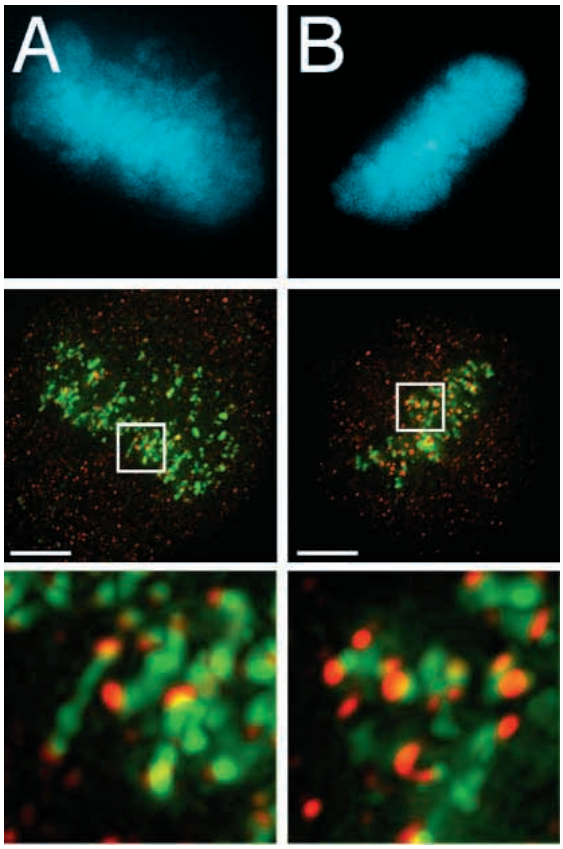

Fig. 8. Loss of tension results in Bub1 recruitment to kinetochores. Projections of deconvolved image stacks showing metaphase HeLa cells stained with Hoechst (blue, top panels), 4B12 (anti-Bub1) and anti-centromere antibodies (red and green respectively in the merged image shown in the middle and bottom panels). The bottom panels show enlarged views of the boxed areas shown in the middle panels. Scale bars represent 5 μm. (A) In the absence of taxol, the metaphase is broad, centromeres are stretched and Bub1 staining at kinetochores is weak. (B) Following 30 minutes of taxol treatment, the metaphase is tight, centromere stretching is reduced and Bub1 staining at kinetochores is increased.

Kinetochores with weaker Bub1 staining are oriented towards the spindle pole

Taken together, the observations presented above are consistent with the notion that when a chromosome becomes mono-oriented the amount of Bub1 detectable at the attached kinetochore diminishes relative to the unattached kinetochore. If this were true, we would expect the kinetochores with weaker Bub1 signal to be closer to the nearest spindle pole. To test this, we analysed untreated prometaphase cells co-stained with antibodies against aurora a, which localises to spindle poles (Bischoff et al., 1998), and Bub1 (Fig. 6A). In general, it does appear that the kinetochores are oriented such that the one exhibiting weaker Bub1 staining is closer to the nearest spindle pole (Fig. 6B). To quantify this, we plotted the K1/K2 Bub1 fluorescence ratio against the inter-kinetochore distance as defined by the K1-to-pole distance minus the K2-to-pole difference (Fig. 6C). If, as predicted, the weaker kinetochore is closer to the nearest spindle pole, the data point for that kinetochore pair will fall above the x-axis. Indeed, 73% of the

points fall above the x-axis and, of the kinetochores displaying significant asymmetry (K1/K2 > 2), six out of eight lie above the x-axis. Thus, these observations suggest that in prometaphase, the kinetochore with a weaker Bub1 signal is indeed oriented towards the spindle pole, consistent with the notion that it is mono-oriented.

Bub1 protein levels decrease rapidly upon return to G_1

The data presented above suggest that kinetochore localisation of Bub1 is significantly more sensitive than that of BubR1 to perturbations in microtubule-kinetochore interactions. To determine whether this difference correlates with the biochemical properties exhibited by these two protein kinases, we analysed Bub1 and BubR1 by western blotting in the presence and absence of microtubule toxins. First, HeLa cells were synchronised at the G_1/S transition then analysed at various times following release (Fig. 7A).

At G_1/S, the amount of Bub1 detectable in HeLa cells is low (Fig. 7A, left panel). As the cells progressed through S phase and into G_2, Bub1 increases by about 10 fold. By 12 hours, when the vast majority of the cells had divided and returned to G_1, the level of Bub1 is dramatically reduced. Bub1 does not disappear at the metaphase-to-anaphase transition or in telophase (Taylor and McKeon, 1997), suggesting that Bub1 levels decline some time in early G_1 then accumulate as cells progress through G_1 into S phase. In contrast, BubR1 is present at G_1/S and increases only marginally as the cells progress into mitosis (Fig. 7A, right panel). Furthermore, whereas Bub1 is virtually undetectable after 12 hours, BubR1 is clearly still present.

Bub1 is phosphorylated in response to spindle damage

Addition of nocodazole six hours after release from G_1/S resulted in the accumulation of cells arrested in mitosis (data not shown). After nine hours, when a significant fraction of the cells were arrested in mitosis, slower-migrating forms of Bub1 and BubR1 are detectable (Fig. 7A). At 12 hours, when virtually all the cells were arrested in mitosis, virtually all of the detectable Bub1 and BubR1 are in the slower-mobility form. Treatment with λ phosphatase or calf intestinal phosphatase results in the disappearance of these slower mobility forms, indicating that they represent phosphorylated forms of Bub1 and BubR1 (Fig. 7B).

Significantly, the phosphorylated form of BubR1 is detectable in the absence of nocodazole (Fig. 7A). In contrast, the phosphorylated form of Bub1 is only detectable in the presence of nocodazole (Fig. 7A). This suggests that although BubR1 is phosphorylated in a normal mitosis, Bub1 is phosphorylated only in the presence of spindle damage. To test this, mitotic HeLa and L929 cells were isolated in the presence or absence of spindle toxins. In protein lysates from mitotic L929 cells obtained in the absence of nocodazole, the slower-mobility form of Bub1 is not detectable (Fig. 7C, top panel), indicating that Bub1 is not significantly phosphorylated during a normal mitosis. However, upon addition of nocodazole for five minutes, the slower-mobility form becomes visible, confirming that Bub1 is phosphorylated in response to spindle damage. In normal mitotic HeLa cells, the slower mobility form of Bub1 is also not detectable (Fig. 7C, middle panel). However, addition of nocodazole or taxol results in the appearance of the phosphorylated form. Interestingly, the band shift observed in the presence of taxol appears larger than that observed following nocodazole treatment.

BubR1 is phosphorylated in the absence of spindle damage

In protein lysates from HeLa cells cultured in the absence of spindle toxins, the slower mobility form of BubR1 is clearly present (Fig. 7C, bottom panel), indicating that BubR1 is phosphorylated during a normal mitosis. The addition of nocodazole or taxol for five minutes does not appear to significantly alter the phosphorylation status of BubR1. After 60 minutes in the absence of nocodazole or taxol, the majority of cells completed mitosis (data not shown) and the majority of BubR1 is dephosphorylated. In contrast, in the presence of nocodazole or taxol, the cells remained in mitosis and the phosphorylated form of BubR1 is still abundant. In summary, these observations indicate that although Bub1 is only phosphorylated in response to spindle damage, BubR1 is phosphorylated during normal mitosis, and spindle damage has little apparent effect.

Bub1 and BubR1 are part of a common complex during mitosis

Bub1 and BubR1 both localise to the same subdomain of the kinetochore during mitosis (Fig. 2). To determine whether Bub1 and BubR1 physically interact, 5F9 and 4B12 were used to affinity purify BubR1 and Bub1 from nocodazole-arrested mitotic cells. When 4B12 was used to immunoprecipitate Bub1, both Bub1 and BubR1 were detectable in the affinity complex (Fig. 7D, lane 1 and 4), indicating that they are indeed part of a common complex in mitosis. When 5F9 was used to affinity purify BubR1, Bub1 was not detectable in the affinity complex (Fig. 7D, lane 3), possibly because 5F9 disrupts the complex or because BubR1 is present in excess relative to Bub1. Significantly, it appears that the phosphorylated form of BubR1 preferentially co-precipitates with Bub1 (Fig. 7D, lane 4). To see if this is indeed the case, we resolved the two isoforms (Fig. 7D, lower panel) and quantified the bands by densitometry. In the BubR1 precipitate, the ratio of phosphorylated to unphosphorylated is about 1.6. In contrast, in the Bub1 precipitate, the ratio of phosphorylated to unphosphorylated BubR1 is about 3.2, thus confirming that the phosphorylated form of BubR1 preferentially co-precipitates with Bub1.

Loss of tension results in Bub1 recruitment to kinetochores

The immunofluorescence data presented above showing Bub1 asymmetry at sister kinetochores suggests that the levels of Bub1 present at kinetochores diminishes following microtubule binding rather than after the application of tension (Fig. 5). However, the observation that Bub1 is rapidly phosphorylated following treatment with taxol for five minutes suggests that Bub1 is sensitive to changes in tension at kinetochores. Therefore to test whether the localisation of Bub1 is also sensitive to changes in tension across the kinetochore, we treated HeLa cells with taxol for 30 minutes, then stained the cells with the 4B12 anti-Bub1 antibody and anti-centromere antibodies (ACA). Cells with metaphase

chromosome alignments were then analysed by deconvolution microscopy. In the absence of taxol, the chromosomes formed a broad metaphase plate and the centromeres appeared stretched (Fig. 8A), consistent with dynamic chromosome oscillations about the metaphase plate and the presence of tension across the centromeres. In contrast, following taxol treatment, the chromosomes formed a tight metaphase plate, and centromere stretching was reduced (Fig. 8B), consistent with oscillation damping and loss of tension. Although Bub1 is detectable at kinetochores in untreated cells (Fig. 8A), consistent with the DLD-1 data presented above (Fig. 1C), kinetochore staining is clearly increased in the taxol-treated cells (Fig. 8B). Thus, reduction in tension across centromeres of chromosomes aligned on the metaphase plate appears to increase kinetochore localisation of Bub1.

DISCUSSION

We have investigated the relative behaviour of Bub1 and BubR1 in human cells, both in terms of their localisation to kinetochores and their phosphorylation status, both during a normal mitosis and in response to spindle perturbation. As described previously by others as well as ourselves, Bub1 and BubR1 first associate with kinetochores during prophase (Taylor and McKeon, 1997; Chan et al., 1998; Jablonski et al., 1998; Taylor et al., 1998). As chromosomes align on the metaphase plate, the intensity of Bub1 and BubR1 at the kinetochores diminishes such that by anaphase only low amounts are detectable. In addition, our data, which shows that Bub1 and BubR1 colocalise to the exact same domain within the kinetochore, is consistent with the notion that, like BubR1 (Jablonski et al., 1998), Bub1 localises to the outer and inner plates of the kinetochore. However, our data show that in prometaphase, Bub1 and BubR1 behave differently: BubR1 is distributed symmetrically between sister kinetochores, whereas Bub1 is frequently asymmetric. This asymmetry appears to be microtubule dependent and the kinetochore with the least Bub1 is usually oriented towards a spindle pole. Furthermore, in response to microtubule depolymerisation, the amount of Bub1 at kinetochores increases dramatically, whereas BubR1 levels remain relatively constant. In addition, although Bub1 and BubR1 have previously been shown to be phospho-proteins (Chan et al., 1999; Schwab et al., 2001; Sharp-Baker and Chen, 2001), our data indicate that although BubR1 is significantly phosphorylated during a normal mitosis, Bub1 is not. However, we show that Bub1 does become rapidly phosphorylated following perturbation of microtubule dynamics at the kinetochore. Consistent with this and another recent report (Skoufias et al., 2001), we show that in response to loss of tension across centromeres, Bub1 re-binds to the kinetochore.

The mouse and human Bub1 proteins were identified as potential homologues of the Bub1 protein kinase discovered in budding yeast (Roberts et al., 1994; Taylor and McKeon, 1997). Mammalian cells were subsequently shown to express a second Bub1-related protein kinase, BubR1 (Chan et al., 1998; Taylor et al., 1998). Why mammals express two Bub1-related protein kinases is a mystery. Although both protein kinases localise to kinetochores during mitosis in a Bub3-dependent manner (Taylor et al., 1998), we show here that sister kinetochores are not equivalent with respect to Bub1 and BubR1 localisation. During prophase, Bub1 accumulates symmetrically at sister kinetochores, but, as the cell then progresses into prometaphase, the localisation of Bub1 often becomes asymmetric. In contrast, BubR1 localises symmetrically to sister kinetochores during prometaphase. This Bub1 asymmetry correlates with the state of microtubules in the cell: stabilisation of microtubules with taxol maintains the asymmetry, whereas deploymerisation of microtubules with nocodazole reduces the asymmetry (Fig. 5; Fig. 7). Furthermore, kinetochores that exhibit asymmetry are typically oriented such that the weaker kinetochore is closer to a spindle pole (Fig. 6). Taken together, these observations suggest that chromosomes exhibiting Bub1 asymmetry are likely to be mono-oriented with the attached, leading kinetochore staining weaker for Bub1 relative to the unattached, lagging kinetochore. In light of this we asked whether the asymmetry might be due to microtubule-mediated masking of the epitope recognised by the 4B12 anti-Bub1 monoclonal antibody. However, both the monoclonal and polyclonal anti-Bub1 antibodies give identical staining patterns in prometaphase cells (Fig. 4), suggesting that the asymmetry is more likely to be due to differences in the relative levels of Bub1 bound to the sister kinetochores.

Significantly, BubR1 is distributed relatively symmetrically between the two sister kinetochores throughout prometaphase, suggesting that whereas Bub1 begins to dissociate following microtubule attachment, BubR1 remains bound. Therefore, relative to BubR1, Bub1 appears to behave more like Mad2, which is not present at kinetochores following microtubule attachment (Waters et al., 1998). Consistent with the notion that Bub1 dissociates from attached kinetochores during prometaphase, although BubR1 remains bound, is the observation that the addition of nocodazole dramatically increases the total amount of Bub1 at kinetochores but has little effect on BubR1 (Fig. 5E). This suggests that in prometaphase, kinetochores have the capacity to re-load Bub1 but not BubR1. This increase in kinetochore-bound Bub1 following nocodazole treatment must be due to loss of microtubule binding rather than loss of tension because taxol treatment does not have the same effect (Fig. 5E).

These observations therefore suggest that localisation of Bub1 to kinetochores is influenced by microtubule attachment. However, the observation that Bub1 is phosphorylated following a five minute taxol treatment suggests that Bub1 is also sensitive to changes in perturbation of microtubule dynamics at the kinetochore (Fig. 7), that is, changes in tension. Interestingly, it was recently shown that the metaphase arrest induced by nanomolar doses of vinblastine results in reassociation of Bub1 with kinetochores (Skoufias et al., 2001). Under these conditions, tension across kinetochores is lost without severing kinetochore-microtubule interactions; hence, the spindle is left intact with chromosomes remaining on the metaphase plate (Jordan et al., 1991). Consistent with this, when we treated HeLa cells with taxol, the chromosomes remained on the metaphase plate, tension across the centromeres was lost and levels of Bub1 at the kinetochore increased (Fig. 8). However, as mentioned above, taxol treatment does not result in re-recruitment of Bub1 to the same extent as nocodazole treatment (Fig. 5).

Taken together, these observations suggest that kinetochores

effectively exhibit three states where the level of bound Bub1 is ‘high’, ‘medium’ or ‘low’. Furthermore, these states correlate with the nature of the interactions between the kinetochores and microtubules. Thus, during normal prophase and prometaphase in the presence of nocodazole, when kinetochores are not attached to microtubules and there is no tension, Bub1 levels are ‘high’. When kinetochores are attached to microtubules but there is little tension, such as during prometaphase in the presence or absence of taxol and during metaphase in the presence of taxol, Bub1 levels are ‘medium’. In prometaphase, Bub1 levels at the unattached kinetochores of mono-oriented chromosomes are still ‘high’, accounting for the asymmetry. When kinetochores are both attached and under tension, such as during a normal metaphase, the Bub1 levels are ‘low’. Therefore, we argue that the amount of Bub1 at kinetochore is governed by both microtubule attachment and tension.

In contrast, our observations suggest that kinetochore localisation of BubR1 is not as sensitive to microtubule attachment as Bub1 is, and therefore the reduction in BubR1 staining that accompanies chromosome alignment (Fig. 1C) is probably due to the application of tension across the kinetochores. This would explain why, in contrast to Bub1, BubR1 does not exhibit asymmetry in prometaphase cells: only when both kinetochores are attached do they come under tension, and then a reduction in the amount of BubR1 at the kinetochore occurs simultaneously. This is in agreement with a recent report that argues that BubR1 localisation does indeed respond to changes in tension but not microtubule attachment (Skoufias et al., 2001).

The notion that Bub1 and BubR1 respond differently to microtubule-kinetochore interactions is supported by our biochemical comparison of the two proteins. Specifically, whereas a significant fraction of BubR1 is phosphorylated in the absence of microtubule toxins, phosphorylation of Bub1 only becomes apparent following spindle damage (Fig. 7). However, when a vertebrate cell enters mitosis, the kinetochores are not attached to the spindle. This does not represent spindle damage, instead it is a normal part of the chromosome-alignment process, and therefore we expect the checkpoint to be active during prometaphase in the absence of spindle toxins. Indeed, expression of a dominant-negative Bub1 mutant and injection of anti-Mad2 antibodies accelerated progression through a normal mitosis (Taylor and McKeon, 1997; Gorbsky et al., 1998). On western blots, there is some smearing behind the Bub1 band, which disappears following spindle damage as the lower-mobility form becomes clearly visible (Fig. 7C, upper panel). We suspect that this indicates that Bub1 is phosphorylated during every mitosis. However, because dephosphorylation probably occurs rapidly during normal spindle assembly, the phosphorylated form only becomes apparent following spindle damage. Interestingly, the change in mobility exhibited by Bub1 appears larger following treatment with taxol relative to nocodazole. Whether Bub1 is phosphorylated at multiple and/or different sites remains to be seen.

Although our observations suggest that Bub1 and BubR1 respond differently to spindle events, these two protein kinases are part of a common complex during mitosis. Significantly, it is the phosphorylated form of BubR1 that immunoprecipitates with Bub1 (Fig. 7). Whether phosphorylation of BubR1 is required for, or a consequence of, association with this complex is not known. However, these observations suggest that Bub1 and BubR1 may be part of a complex that acts as a sensor to integrate information about the status of kinetochore-microtubule interactions into a single signal that is then relayed to downstream cell cycle effectors (Nasmyth, 1999; Shah and Cleveland, 2000).

S.S.T. and Y.W. are extremely grateful to Frank McKeon (Harvard Medical School) for support during the early phase of this work. We also thank Keith Gull, Don Cleveland, Nick Keen and Howard Green for antibodies and cell lines. The DeltaVision microscope was obtained with funds from a BBSRC Bioimaging grant to Keith Gull and Iain Hagan. We are grateful to other members of the Taylor Laboratory, especially Vicky Johnson for advice and comments on the manuscript. DH, CJM and SST are supported by the BBSRC with additional funding from the Breast Cancer Campaign, The Leverhulme Trust, The Royal Society and Glaxo SmithKline.

REFERENCES

Amon, A. (1999). The spindle checkpoint. *Curr. Opin. Genet. Dev.* **9**, 69-75.

Basu, J., Logarinho, E., Herrmann, S., Bousbaa, H., Li, Z., Chan, G. K., Yen, T. J., Sunkel, C. E. and Goldberg, M. L. (1998). Localization of the *Drosophila* checkpoint control protein Bub3 to the kinetochore requires Bub1 but not Zw10 or Rod. *Chromosoma* **107**, 376-385.

Basu, J., Bousbaa, H., Logarinho, E., Li, Z., Williams, B. C., Lopes, C., Sunkel, C. E. and Goldberg, M. L. (1999). Mutations in the essential spindle checkpoint gene bub1 cause chromosome missegregation and fail to block apoptosis in *Drosophila*. *J. Cell Biol.* **146**, 13-28.

Bischoff, J. R., Anderson, L., Zhu, Y., Mossie, K., Ng, L., Souza, B., Schryver, B., Flanagan, P., Clairvoyant, F., Ginther, C. et al. (1998). A homologue of *Drosophila* aurora kinase is oncogenic and amplified in human colorectal cancers. *EMBO J.* **17**, 3052-3065.

Brady, D. M. and Hardwick, K. G. (2000). Complex formation between Mad1p, Bub1p and Bub3p is crucial for spindle checkpoint function. *Curr. Biol.* **10**, 675-678.

Campbell, M. S. and Gorbsky, G. J. (1995). Microinjection of mitotic cells with the 3F3/2 anti-phosphoepitope antibody delays the onset of anaphase. *J. Cell Biol.* **129**, 1195-1204.

Chan, G. K., Schaar, B. T. and Yen, T. J. (1998). Characterization of the kinetochore binding domain of CENP-E reveals interactions with the kinetochore proteins CENP-F and hBUBR1. *J. Cell Biol.* **143**, 49-63.

Chan, G. K., Jablonski, S. A., Sudakin, V., Hittle, J. C. and Yen, T. J. (1999). Human BUBR1 is a mitotic checkpoint kinase that monitors CENP-E functions at kinetochores and binds the cyclosome/APC. *J. Cell Biol.* **146**, 941-954.

Chen, R.-H., Waters, J. C., Salmon, E. D. and Murray, A. W. (1996). Association of spindle assembly checkpoint component XMAD2 with unattached kinetochores. *Science* **274**, 242-246.

Chen, R. H., Shevchenko, A., Mann, M. and Murray, A. W. (1998). Spindle checkpoint protein Xmad1 recruits Xmad2 to unattached kinetochores. *J. Cell Biol.* **143**, 283-295.

Cooke, C. A., Schaar, B., Yen, T. J. and Earnshaw, W. C. (1997). Localization of CENP-E in the fibrous corona and outer plate of mammalian kinetochores from prometaphase through anaphase. *Chromosoma* **106**, 446-455.

Fang, G., Yu, H. and Kirschner, M. W. (1998). The checkpoint protein MAD2 and the mitotic regulator CDC20 form a ternary complex with the anaphase-promoting complex to control anaphase initiation. *Genes Dev.* **12**, 1871-1883.

Gorbsky, G. J. and Ricketts, W. A. (1993). Differential expression of a phosphoepitope at the kinetochores of moving chromosomes. *J. Cell Biol.* **122**, 1311-1321.

Gorbsky, G. J., Chen, R. H. and Murray, A. W. (1998). Microinjection of antibody to Mad2 protein into mammalian cells in mitosis induces premature anaphase. *J Cell Biol.* **141**, 1193-1205.

Hardwick, K. G., Johnston, R. C., Smith, D. L. and Murray, A. W. (2000). MAD3 encodes a novel component of the spindle checkpoint which interacts with Bub3p, Cdc20p, and Mad2p. *J. Cell Biol.* **148**, 871-882.

Hoyt, M. A., Totis, L. and Roberts, B. T. (1991). *S. cerevisiae* genes required

for cell cycle arrest in response to loss of microtubule function. *Cell* **66**, 507-517.

Hwang, L. H., Lau, L. F., Smith, D. L., Mistrot, C. A., Hardwick, K. G., Hwang, E. S., Amon, A. and Murray, A. W. (1998). Budding yeast Cdc20: a target of the spindle checkpoint. *Science* **279**, 1041-1044.

Jablonski, S. A., Chan, G. K., Cooke, C. A., Earnshaw, W. C. and Yen, T. J. (1998). The hBUB1 and hBUBR1 kinases sequentially assemble onto kinetochores during prophase with hBUBR1 concentrating at the kinetochore plates in mitosis. *Chromosoma* **107**, 386-396.

Jordan, M. A., Thrower, D. and Wilson, L. (1991). Mechanism of inhibition of cell proliferation by Vinca alkaloids. *Cancer Res.* **51**, 2212-2222.

Kim, S. H., Lin, D. P., Matsumoto, S., Kitazono, A. and Matsumoto, T. (1998). Fission yeast Slp1: an effector of the Mad2-dependent spindle checkpoint. *Science* **279**, 1045-1047.

Li, R. and Murray, A. W. (1991). Feedback control of mitosis in budding yeast. *Cell* **66**, 519-531.

Li, X. and Nicklas, R. B. (1995). Mitotic forces control a cell-cycle checkpoint. *Nature* **373**, 630-632.

Li, Y. and Benezra, R. (1996). Identification of a human mitotic checkpoint gene: hsMAD2. *Science* **274**, 246-248.

Nasmyth, K. (1999). Separating sister chromatids. *Trends Biochem. Sci.* **24**, 98-104.

Nicklas, R. B., Ward, S. C. and Gorbsky, G. J. (1995). Kinetochore chemistry is sensitive to tension and may link mitotic forces to a cell cycle checkpoint. *J. Cell Biol.* **130**, 929-939.

Nicklas, R. B. (1997). How cells get the right chromosomes. *Science* **275**, 632-637.

Rieder, C. L., Schultz, A., Cole, R. and Sluder, G. (1994). Anaphase onset in vertebrate somatic cells is controlled by a checkpoint that monitors sister kinetochore attachment to the spindle. *J. Cell Biol.* **127**, 1301-1310.

Rieder, C. L., Cole, R. W., Khodjakov, A. and Sluder, G. (1995). The checkpoint delaying anaphase in response to chromosome monoorientation is mediated by an inhibitory signal produced by unattached kinetochores. *J. Cell Biol.* **130**, 941-948.

Roberts, B. T., Farr, K. A. and Hoyt, M. A. (1994). The *Saccharomyces cerevisiae* checkpoint gene BUB1 encodes a novel protein kinase. *Mol. Cell. Biol.* **14**, 8282-8291.

Schaar, B. T., Chan, G. K., Maddox, P., Salmon, E. D. and Yen, T. J. (1997). CENP-E function at kinetochores is essential for chromosome alignment. *J. Cell Biol.* **139**, 1373-1382.

Schwab, M. S., Roberts, B. T., Gross, S. D., Tunquist, B. J., Taieb, F. E., Lewellyn, A. L. and Maller, J. L. (2001). Bub1 is activated by the protein kinase p90(Rsk) during *Xenopus* oocyte maturation. *Curr. Biol.* **11**, 141-150.

Shah, J. V. and Cleveland, D. W. (2000). Waiting for anaphase: Mad2 and the spindle assembly checkpoint. *Cell* **103**, 997-1000.

Sharp-Baker, H. and Chen, R. H. (2001). Spindle checkpoint protein bub1 is required for kinetochore localization of mad1, mad2, bub3, and cenp-e, independently of its kinase activity. *J. Cell Biol.* **153**, 1239-1250.

Skoufias, D. A., Andreassen, P. R., Lacroix, F. B., Wilson, L. and Margolis, R. L. (2001). Mammalian mad2 and bub1/bubR1 recognize distinct spindle-attachment and kinetochore-tension checkpoints. *Proc. Natl. Acad. Sci. USA* **98**, 4492-4497.

Taylor, S. S. and McKeon, F. (1997). Kinetochore localization of murine Bub1 is required for normal mitotic timing and checkpoint response to spindle damage. *Cell* **89**, 727-735.

Taylor, S. S., Ha, E. and McKeon, F. (1998). The human homologue of Bub3 is required for kinetochore localization of Bub1 and a Mad3/Bub1-related protein kinase. *J. Cell Biol.* **142**, 1-11.

Waters, J. C., Chen, R. H., Murray, A. W. and Salmon, E. D. (1998). Localization of Mad2 to kinetochores depends on microtubule attachment, not tension. *J. Cell Biol.* **141**, 1181-1191.

Wood, K. W., Sakowicz, R., Goldstein, L. S. and Cleveland, D. W. (1997). CENP-E is a plus end-directed kinetochore motor required for metaphase chromosome alignment. *Cell* **91**, 357-366.

Woods, A., Sherwin, T., Sasse, R., MacRae, T. H., Baines, A. J. and Gull, K. (1989). Definition of individual components within the cytoskeleton of *Trypanosoma brucei* by a library of monoclonal antibodies. *J. Cell Sci.* **93**, 491-500.

Yao, X., Anderson, K. L. and Cleveland, D. W. (1997). The microtubule-dependent motor centromere-associated protein E (CENP- E) is an integral component of kinetochore corona fibers that link centromeres to spindle microtubules. *J. Cell Biol.* **139**, 435-447.

Yao, X., Abrieu, A., Zheng, Y., Sullivan, K. F. and Cleveland, D. W. (2000). CENP-E forms a link between attachment of spindle microtubules to kinetochores and the mitotic checkpoint. *Nat. Cell Biol.* **2**, 484-491.

Zirkle, R. E. (1970). Ultraviolet-microbeam irradiation of newt-cell cytoplasm: spindle destruction, false anaphase, and delay of true anaphase. *Radiat. Res.* **41**, 516-537.